A numerical scheme for various nonlinear forces, including collisions, which does not require an iterative root finder

A NUMERICAL SCHEME FOR VARIOUS NONLINEAR FORCES, INCLUDING COLLISIONS, WHICH DOES NOT REQUIRE AN ITERATIVE ROOT FINDER

Michele Ducceschi

Acoustics and Audio Group,
University of Edinburgh
Edinburgh, UK
michele.ducceschi@ed.ac.uk

ABSTRACT

Nonlinear forces are ubiquitous in physical systems, and of prominent importance in musical acoustics. Though many models exist to describe such forces, in most cases the associated numerical schemes rely on iterative root finding methods, such as Newton-Raphson or gradient descent, which are computationally expensive and which therefore could represent a computational bottleneck. In this paper, a model for a large class of nonlinear forces is presented, and a novel family of energy-conserving finite difference schemes given. The schemes only require the evaluation of the roots of a quadratic function. A few applications in the lumped case are shown, and the robustness and accuracy of the scheme tested.

1. INTRODUCTION

In many musical instruments, collisions and contact forces are involved at various levels in the mechanism of sound production [1]. The interaction of strings with a bow, a membrane (like in the snare drum), a mallet, a finger or a fretboard are all examples of contact forces. Collisions of the reed in wind instruments have a major impact on the perceived tonal quality. Prepared piano string (coupled to rattling elements) are yet another example of such collisions. Outside of musical acoustics, collisions represent an important field of study in robotics [2], and of course computer graphics [3, 4]. The models employed to describe all the above forces are necessarily nonlinear, and hence they represent a challenge in terms of numerical simulation. Although many methods have been used to simulate some specific examples of collisions (including digital waveguides [5], modal methods [6, 7], and time stepping methods [8]), a fairly recent general framework was proposed in order to simulate a large class of collisions and contact forces [1]. In this framework, the forces are generated by a potential which takes the form of some kind of power law, depending on one stiffness coefficient, and one exponent. Such framework allows to simulate collisions of two lumped objects (like a mass and a spring), of one lumped and one distributed object (like a mallet and a string), and even of two distributed systems (like a string and a membrane). For very stiff collisions, the forces are generated by a spurious interpenetration, which can be made as small as possible by increasing the stiffness coefficient. Though extremely versatile, the associated energy-conserving numerical schemes rely on iterative root finding algorithms, such as Newton-Raphson, which is most cases represent a computational bottleneck. In this paper, a novel family of finite difference schemes is proposed for the lumped case, which do not require an iterative root finding method. It should be mentioned that previous works (see for example [9, 10]) do present numerical schemes able to simulate collisions without iterative root finding algorithms. However, this was showed only in the case of linear response of the barrier with the spurious interpenetration. In this paper, the proposed schemes work for a class of nonlinear potentials. At each update the nonlinear force can be calculated by simply finding the roots of a quadratic function, which basically involves the evaluation of a single square root. In section 2, the model is presented in the form of an ordinary differential equation, and the forms of the potentials given. Finite difference schemes are presented in section 3, derived from a given Hamiltonian depending on one scalar parameter. Boundedness of the energy will be shown, along with a discussion of the realness of the roots of the quadratic. Tests for accuracy are presented at this point. Finally, section 4 shows a few applications of interest.

2. MODEL EQUATIONS

In the course of this paper, the displacement $u(t)$ of a particle of mass M is described by an ordinary differential equation of the following form

$$M\ddot{u} = -\phi'(u) = -\frac{\dot{\phi}(u)}{\dot{u}}, \tag{1}$$

where the last equality was obtained by means of the chain rule. In the equation, the particle is assumed to be subjected to a force described by the potential $\phi(u)$. By multiplying both sides of the equation by $\dot{u}$ the following energy identity is obtained

$$\frac{\mathrm{d}}{\mathrm{d}t}\left(\frac{M}{2}\dot{u}^2 + \phi(u)\right) \triangleq \frac{\mathrm{d}}{\mathrm{d}t}\mathfrak{H} = 0 \quad \rightarrow \quad \mathfrak{H} = \mathfrak{H}_0, \tag{2}$$

and hence the energy $\mathfrak{H}$ is non-negative if and only if $\phi(u) \geq 0\ \forall u$. Various potentials satisfy such requirement. Specific forms of interest here are the following

$$\phi(u) = \frac{K}{\alpha+1}u^{\alpha+1}, \qquad \alpha = 1, 3, 5, ... \tag{3a}$$

$$\phi(u) = \frac{K}{\alpha+1}[u-h]_+^{\alpha+1}, \quad \alpha \in \mathbb{R}, \alpha > 1 \tag{3b}$$

$$\phi(u) = \frac{K}{\alpha+1}[|u|-h]_+^{\alpha+1}, \quad \alpha \in \mathbb{R}, \alpha > 1 \tag{3c}$$

In the equations, the symbol $[x]_+$ denotes the positive part, i.e. $2[x]_+ \triangleq x + |x|$. The constant K is a stiffness coefficient. The forces originated by such potentials are depicted in Fig. 1. In musical acoustics, though often for distributed systems, these potentials are used in modelling large-amplitude nonlinearities, contact nonlinearities (such as the hammer-string interaction), rattling elements, and other important nonlinear interactions [11].

From (2), one finds immediately a bound on the growth of the solution, i.e.

$$(\dot{u})^2 \leq \frac{2\mathfrak{H}_0}{M}, \tag{4}$$

where $\mathfrak{H}_0$ (a constant) is the total energy.

3. FINITE DIFFERENCE SCHEMES

Solutions to (1) are now sought in terms of appropriate finite difference schemes, upon the introduction of a sample rate f_s and the associated time step $k = 1/f_s$. The solution is evaluated at the discrete times nk, where $n \in \mathbb{Z}^+$, and is denoted u^n. Finite difference operators are introduced as:

- backward and forward shift operators
  $e_{t-}u^n \triangleq u^{n-1},\ e_{t+}u^n \triangleq u^{n+1}$
- backward, centered and forward first time derivatives
  $\delta_{t-} \triangleq \frac{1}{k}(1-e_{t-}), \delta_{t\cdot} \triangleq \frac{1}{2k}(e_{t+}-e_{t-}), \delta_{t+} \triangleq \frac{1}{k}(e_{t+}-1)$
- averaging operators
  $\mu_{t+} \triangleq \frac{1}{2}(1+e_+),\ \mu_{t-} \triangleq \frac{1}{2}(1+e_-),\ \mu_{t-}^{(s)} \triangleq s+(1-s)e_{t-}\ (s \in \mathbb{R})$
- second time derivative
  $\delta_{tt} \triangleq \delta_{t+}\delta_{t-} = \frac{1}{k^2}(e_{t+}-2+e_{t-})$

In order to derive a finite difference scheme, a general form for the Hamiltonian is given here in terms of the generalised averaging operator defined above, as

$$\mathfrak{h}^{n-1/2} = \frac{M}{2}(\delta_{t-}u^n)^2 + \mu_{t-}^{(s)}\phi(u^n). \tag{5}$$

Notice that the particular choice $s = \frac{1}{2}$ leads to the Hamiltonian considered in [1], whose associated finite difference scheme is second-order accurate, and whose update requires an iterative root finding method such as the Newton-Raphson algorithm.

In this work, the potential energy is Taylor-expanded around the point u^{n-1} up to second order, giving

$$\mu_{t-}^{(s)}\phi(u^n) \approx \phi(u^{n-1}) + s(u^n-u^{n-1})\phi'(u^{n-1}) + s\frac{(u^n-u^{n-1})^2}{2}\phi''(u^{n-1}) \triangleq P_{n-1,n}^{(s)} \tag{6}$$

Hence, the Hamiltonian considered in this work, depending on the parameter s, is

$$\mathfrak{h}^{n-1/2} = \frac{M}{2}(\delta_{t-}u^n)^2 + P_{n-1,n}^{(s)} \tag{7}$$

3.1. Boundedness of Potential Energy

The potential energy defined in (6) is a parabola in $u^n - u^{n-1}$. Moreover, for the potentials considered in (3) the following identities hold

$$\phi'(u) = (\alpha+1)\frac{\phi(u)}{\bar{u}}, \quad \phi''(u) = \alpha(\alpha+1)\frac{\phi(u)}{\bar{u}^2}, \tag{8}$$

where

$$\bar{u} \triangleq u \qquad \text{for (3a)}$$
$$\bar{u} \triangleq u-h \qquad \text{for (3b)}$$
$$\bar{u} \triangleq \frac{|u|-h}{\text{sign}(u)} \qquad \text{for (3c)}$$

Hence, one has

$$P_{n-1,n}^{(s)} = \phi(u^{n-1})\left[1+s(\alpha+1)x + s(\alpha+1)\alpha\frac{x^2}{2}\right] \tag{9}$$

where

$$x \triangleq \frac{u^n-u^{n-1}}{\bar{u}^{n-1}}. \tag{10}$$

The potential energy will be non-negative if and only if the discriminant of the quadratic above is less than or equal to zero, i.e.

$$s^2(\alpha+1)^2 - 2s(\alpha+1)\alpha \leq 0. \tag{11}$$

This is a parametric inequality that must be evaluated according the sign of s and $(\alpha+1)$. Notice that, for the potentials in (3), one must check that the solutions are valid $\forall\alpha \geq 1$. This gives

$$0 < s \leq 1. \tag{12}$$

Such values will ensure that $P_{n-1,n}^{(s)}$ is non-negative, and therefore that the discrete Hamiltonian (7) is non-negative, $\forall\alpha \geq 1$.

In this case, boundedness of the potential energy can be achieved for values of s which do not guarantee non-negativity of the potential energy. In fact, given the particular form of the potential energy (9), if the coefficient multiplying x^2 is positive, then the parabola will always have a minimum regardless of the value of u^{n-1}, and hence $\forall n$ (remember that ϕ is non-negative by definition). Such coefficient is $s(\alpha+1)\alpha$ and, because in this work $\alpha \geq 1$, the potential energy will then be bounded from below $\forall s \geq 0$. The bound depends on the intial conditions, and tends to zero as the sampling rate is increased, see also Fig. 5.

Summarising, in this work

$$s > 0, \quad \alpha \geq 1 \tag{13}$$

with the particular case $0 < s \leq 1$ guaranteeing non-negativity of the potential energy.

3.2. Energy conservation. Finite difference scheme

A finite difference scheme can be derived from the Hamiltonian above by imposing

$$\delta_{t+}\mathfrak{h}^{n-1/2} = 0. \tag{14}$$

Before deriving the scheme, notice that when the potential energy is non-negative, one immediately finds a bound similar to (4), i.e.

$$(\delta_{t-}u^n)^2 \leq \frac{2\mathfrak{h}_0}{M}, \tag{15}$$

When the potential energy is not positive, but bounded from below, such inequality is true up to a correction of the order of k^2. Upon the introduction of the variable $y \triangleq u^{n+1}-u^{n-1}$, the scheme is

$$Ay + B + \frac{C}{y} = 0, \tag{16}$$

where the coefficients A, B, C depend on previous values, and are given as

$$A = \frac{M}{k^2} + s\phi''(u^n)$$
$$B = -\frac{2M}{k^2}(u^n-u^{n-1}) + 2s\phi'(u^n) + 2s(u^{n-1}-u^n)\phi''(u^n)$$
$$C = 2P_{n,n-1}^{(s)} - 2P_{n-1,n}^{(s)}$$

Under the assumption $y \neq 0$, the scheme can be written as a quadratic in y, i.e.

$$Ay^2 + By + C = 0. \tag{17}$$

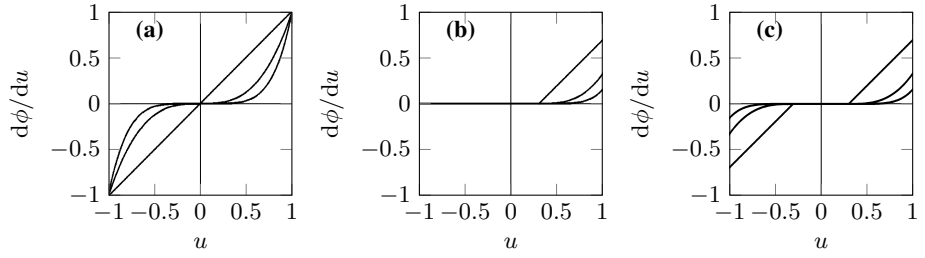

Figure 1: Nonlinear forces. (a): nonlinear power law, as per (3a), for $K = 1, \alpha = 1, 3, 5$. (b): one-sided power law, as per (3b), for $K = 1, \alpha = 1, 1.7, 2.8$, $h = 0.2$. (c): center limited power law, as per (3c), for $K = 1, \alpha = 1, 1.7, 2.8$, $h = 0.3$.

3.3. Existence and Uniqueness

Scheme (17) requires the knowledge of the roots of a quadratic function at each update, and is thus very attractive numerically as one may employ the well-known closed-form solution for quadratics instead of a nonlinear root finding algorithm. However, existence of the roots must be checked, and a condition on existence must be given. Also, if the roots exist, they come in pairs, posing a question on uniqueness. Existence is first checked, and the question of uniqueness is discussed later.

3.3.1. Existence

The condition to impose is

$$\Delta^{(\alpha)} \triangleq B^2 - 4AC \geq 0. \tag{18}$$

The discriminat $\Delta^{(\alpha)}$ depends on the particular choice of the exponent α. Existence of the solutions will be checked for $\Delta^{(1)}$, and a discussion for larger values of α will be given later. Also, because potential (3b) and (3c) depend on the positive part of their argument, various cases must be discussed. These are

1. $\phi(u^n) = \phi(u^{n-1}) = 0$. This scenario corresponds to the particle not being in contact with the barrier/spring. In this case $C = 0$ and therefore $\Delta^{(1)} \geq 0$.
2. $\phi(u^{n-1}) > 0, \phi(u^n) = 0$. This scenario corresponds to the particle moving away from the barrier/spring, and this gives $C = -2P^{(s)}_{n-1,n}$ and because $A > 0$ one has $-4AC > 0$ and therefore $\Delta^{(1)} \geq 0$ (remember that $P^{(s)}_{n-1,n}$ under condition (12) is positive-definite).
3. $\phi(u^n) > 0, \phi(u^{n-1}) = 0$. This scenario corresponds to the particle colliding against the barrier/spring, and must be checked.
4. $\phi(u^n) > 0, \phi(u^{n-1}) > 0$. This scenario corresponds to (3a), as well as to (3b), (3c) when the particle and the barrier/spring are in full contact (spurious interpenetration). This case must also be discussed.

Hence, the only cases to discuss are 3 and 4.
Case 3. Upon the definition of $\bar{K} = K/M$ and $u_h = u - h$, this case gives

$$\Delta^{(1)} = \frac{A}{k^2}(u_h^{n-1})^2 + (u_h^n)^2\left[\frac{1}{k^4} - A\bar{K} + sA\bar{K}\right] - \frac{2}{k^2}Au_h^n u_h^{n-1}.$$

Remembering that for this case $u_h^n > 0$, $u_h^{n-1} < 0$ one can find a *sufficient* condition for positivenenss by imposing

$$-A\bar{K} + sA\bar{K} \geq 0, \quad \rightarrow \quad s \geq 1.$$

Case 4. Using again the same definition of $\bar{K}$ and u_h, one has (up to a positive constant of proportionality)

$$\Delta^{(1)} = \bar{K}s^2(u_h^{n-1})^2 + \frac{1}{k^2}(\delta_{t-}u_h^n)^2 - 2\left[\frac{s}{k}\bar{K}u_h^{n-1} + Ak\left(\frac{\bar{K}}{2} - s\bar{K}\right)(\mu_{t-}u_h^n)\right](\delta_{t-}u_h^n)$$

Hence $\Delta^{(1)}$ is a parabola in $(\delta_{t-}u_h^n)$. Also, for $s \geq \frac{1}{2}$, $\Delta^{(1)}$ could take on negative values only if $u_h^{n-1} > u_h^n$. Under such assumptions, the discriminant of the parabola is calculated, and again the requirement is that such discriminant be negative. Using the fact that $u_h^{n-1} > u_h^n$ one finds a *sufficient* condition on the time step to be

$$k^2 \leq \frac{s + \frac{1}{2}}{\bar{K}s(s - \frac{1}{2})} \quad \text{for } s > \frac{1}{2}$$

$$\text{unconditionally positive} \quad \text{for } s = \frac{1}{2}.$$

Summarising

- for potential (3a), $\Delta^{(1)}$ will be unconditionally positive for $s = \frac{1}{2}$, otherwise a *sufficient* condition can be given as: $s > \frac{1}{2}$, $k^2 \leq \frac{s+\frac{1}{2}}{\bar{K}s(s-\frac{1}{2})}$
- for potentials (3b), (3c), a *sufficient* condition can be given as: $s \geq 1$, $k^2 \leq \frac{s+\frac{1}{2}}{\bar{K}s(s-\frac{1}{2})}$

3.3.2. Uniqueness

Assuming realness of the roots of (17), at each time step one has to choose either y_+ or y_-, defined as

$$y_\pm = \frac{-B \pm \sqrt{\Delta^{(a)}}}{2A}. \tag{19}$$

The choice is made according to the following rule

- if $B \geq 0$ choose y_-
- if $B < 0$ choose y_+

To understand why this rule holds, consider the case of a free particle, i.e. for which the potential is zero at all times. In this case, scheme (17) reduces to

$$Ay^2 + By = 0, \tag{20}$$

with solutions

$$y_\pm = \frac{-B \pm \sqrt{B^2}}{2A} = \frac{-B \pm |B|}{2A}, \tag{21}$$

but because the solution $y = 0$ is ruled out, one recovers the rule above.

3.3.3. *Comments on existence, $\Delta^{(\alpha>1)}$ and bounds*

In this subsection, some comments are given regarding the realness of the roots of (17), for $\alpha > 1$. A discussion on the sign of $\Delta^{(\alpha>1)}$ is somewhat complicated by the fact that u_h^n, u_h^{n-1} appear nonlinearly with rational exponents, or with high-order powers, and hence it is difficult to carry on a study of the sign of $\Delta^{(\alpha>1)}$ along the same lines as $\Delta^{(1)}$. A possible procedure is to consider a parametric study of the function $\mathrm{d}\Delta^{(\alpha)}/\mathrm{d}\alpha$, and hence find conditions on maxima and minima of $\Delta^{(\alpha)}$ for the various signs of u_h^n, u_h^{n-1}. This rigorous approach, though desirable, is somewhat lengthy and perhaps beyond the scope of the current work. A less rigorous, though revealing approach is to make use of brute force, i.e. to launch many simulations testing out large portions of the parameter space, and to empirically verify the robustness of the algorithm.

In Fig. 2, the scheme is checked for potential (3a), for $s = \frac{1}{2}, 1, 3$. The particle has mass $M = 1$ kg, and the spring has stiffness $K = 10^3$. Each case presents two subcases, i.e. standard and very high initial velocities (1 m/s, 20 m/s). The figures report the minimum of $\Delta^{(\alpha)}$, for $\alpha \in [1, 3, 5, 7, 9, 11, 13]$. Each colour is associated with a different time step. Missing points correspond to simulations returning complex roots. The time steps are chosen as $k_i = \frac{2^{i-2}}{\sqrt{K}}$, for $i = 1, 2, 3, 4$. Notice that k_3 is the limit of stability of the classic second-order accurate scheme for the simple harmonic oscillator, (22). For $s = \frac{1}{2}$, $\Delta^{(1)}$ is always positive, in accordance with the previous observation that for such value of s, $\Delta^{(1)}$ is unconditionally positive. However, the scheme is quite poorly behaved for higher values of α, especially under extreme initial conditions. Things look much better for $s = 1$, where the scheme always returns real roots for $v = 1$ m/s, as well as for $v = 20$ m/s when $\alpha = 1, 3$, $k = k_1, k_2, k_3$. When $s = 3$, the scheme always returns real roots, for both $v = 1$ and $v = 20$ m/s. In fact, in this case the minimum of $\Delta^{(\alpha)}$ seems to have reached an asymptote. Notice that the values of α selected for the figures are unreasonably high for applications in musical acoustics (in practice, one always chooses $1 \leq \alpha \leq 3$). However, it is remarkable that the scheme still works under such extreme conditions, at no extra computational cost.

A discussion for potentials (3b) and (3c) is not reported here, but the same conclusions apply.

Similar plots suggest that computability is increased as the parameter s is increased.

Summarising, empirical observations suggest that scheme (17) gives real roots in the following cases

- conditional realness for $1 \leq \alpha \leq 3$ if $s = 1$, the condition being (at worst) $k \leq \frac{2}{\sqrt{K}}$
- unconditional realness $\forall \alpha \geq 1$, if $s > 2$

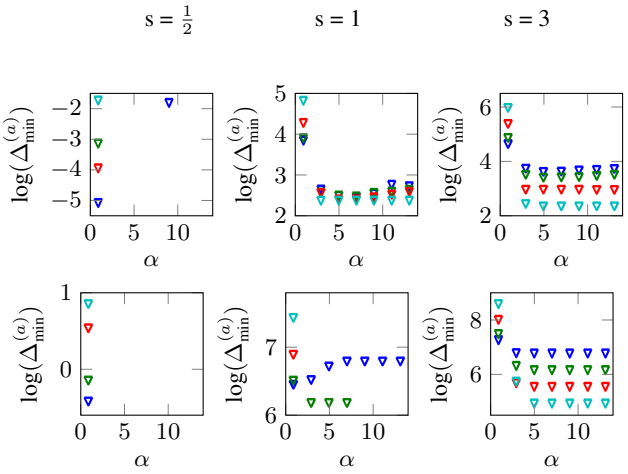

Figure 2: Computability of proposed scheme: values of $\Delta^{(\alpha)}$ for the selected values of the free parameter s. Missing points correspond to complex roots. For the simulations, $M = 1$ kg, $K = 10^3$, $\alpha \in [1, 3, 5, 7, 9, 11, 13]$. Time steps chosen as $k_1 = \sqrt{\frac{M}{4K}}$ (dark blue), $k_2 = \sqrt{\frac{M}{K}}$ (green), $k_3 = \sqrt{\frac{4M}{K}}$ (red), $k_4 = \sqrt{\frac{16M}{K}}$ (light blue). Notice that k_3 is the largest timestep allowed for the classic simple harmonic oscillator scheme, (22). Top row: initial velocity $v_0 = 1$ m/s, initial displacement $u_0 = -1$ mm. Bottom row: initial velocity $v_0 = 20$ m/s, initial displacement $u_0 = -1$ mm.

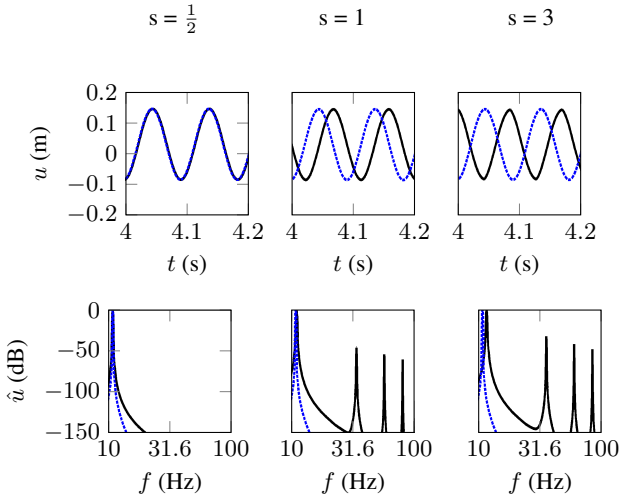

Figure 3: Simple harmonic oscillator. Comparison of current scheme, for potential (3a) with $\alpha = 1$ (solid line), and classic scheme (22) (dashed line). Top row: time domain. Bottom row: frequency domain. Free parameter s chosen as indicated on top. Natural frequency of the oscillator is $f_0 = 11$ Hz. Sampling rate chosen as $f_s = 2300$ Hz. Initial conditions: $v_0 = 0.5$ m/s, $u_0 = -0.1$ m.

4. APPLICATIONS

Scheme (17) is now tested against various benchmark schemes. First, the problem of the simple harmonic oscillator is considered. Then the dynamics of a particle colliding against a stiff barrier is studied, followed by the cubic oscillator.

4.1. Simple Harmonic Oscillator

In order to assess the properties of scheme (17), the simple harmonic oscillator is numerically simulated under various choices of the parameter s, and comparated against a second-order accurate benchmark scheme (see [11] for details) given by

$$u^{n+1} = (2 - k^2\bar{K})u^n - u^{n-1}, \qquad k \leq \frac{2}{\sqrt{\bar{K}}}. \tag{22}$$

Fig. 3 presents a few such comparisons, for $s = \frac{1}{2}, 1, 3$. The question of accuracy for the current scheme is an interesting one. For the case of the simple harmonic oscillator considered here there are two sources of error: the first one is numerical dispersion (in fact, this is known as phase errors for the lossless case); the second one is due to the truncation of the Taylor series (6) to second order. Frequency domain analysis (i.e. z-transform techinques) are in this case out of hand, because for scheme (17) the values of the solution at the times $n+1, n, n-1$ appear nonlinearly even under linear conditions for the potential (3a).

There are some interesting facts about Fig. 3. First of all, the scheme is less and less accurate as s is increased. This observation is somewhat in contrast with the observation on existence of the roots of (17) (see also Fig. 2): there is a trade-off between accuracy and computability. In particular, for $s = 1, 3$ the fundamental frequency is higher than the one obtained with the classic scheme, resulting in the sinusoids shifting apart in the time domain. The second interesting fact is that $\forall s \neq \frac{1}{2}$ the simulated system is *nonlinear*, even though the model equation of the simple harmonic oscillator is completely linear. Nonlinearities appear as odd harmonics in the spectra of the cases for $s = 1, 3$. Even though such peaks are much lower in energy than the fundamental (for $s = 1$ the second harmonic is lower than 60 dB in amplitude), as s is increased they become more and more prominent. However, the amplitude of such peaks is insensitive to the initial conditions (in particular they do not grow when higher inital velocities or displacements are used).

It is of course the case to point out that scheme (17) is probably not very well suited for the problem of the simple harmonic oscillator, at least $\forall s \neq \frac{1}{2}$. This is because in general the scheme does not make a distinction between linear and nonlinear cases, so long as the potential ϕ is positive-definite and therefore the properties of existence of the roots and of positiveness of the discrete Hamiltonian are preserved. In other words, the scheme offers a general way to treat a large class of nonlinear problems, including the linear case as some sort of "sub-case", but where the scheme remains nonlinear.

4.2. Colliding Mass

In this subsection the dynamics of a colliding mass against a stiff barrier is simulated. Fig. 4 presents the comparison of the current scheme, under various choices of the parameter s, and a benchmark scheme presented in [1], which reads

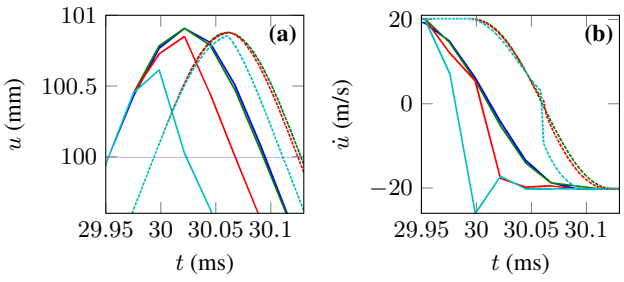

Figure 4: Collision of a fast particle against a stiff barrier. Comparison of benchmark scheme (blue) (23) and proposed scheme, for $s = \frac{1}{2}$ (green), $s = 1$ (red), $s = 3$ (cyan). Particle has mass $M = 1$ kg, and is started at $u_0 = -0.5$ m with initial velocity $v_0 = 20$ m/s against a barrier located at $h = 0.1$ m; barrier parameters are $K = 5 \cdot 10^9$, $\alpha = 1.3$. For both figures, solid lines and dashed lineds are obtained using, respectively, $f_s = 44100$ and $f_s = 441000$. (a): Particle displacement during collision (spurious interpenetration). (b): Particle velocity during collision.

$$y + \frac{k^2}{My}\left[\phi(y + u^{n-1}) - \phi(u^{n-1})\right] + 2u^{n-1} - 2u^n = 0, \tag{23}$$

where $y \triangleq u^{n+1} - u^{n-1}$. The scheme is second order accurate, and unconditionally stable provided that one is able to calculate y which appears implicitly in the argument of ϕ. In order to solve for such scheme, one must employ a nonlinear root finding algorithm, such as Newton-Raphson. Considering Fig. 4, it is seen that the current scheme departs more and more from the benchmark scheme as s is increased; this observation is consistent with what was already noted for the case of the harmonic oscillator. In particular, for $s = \frac{1}{2}$ the proposed scheme is virtually undistinguishable from the benchmark scheme, whereas for $s = 1, 3$ differences can be noticed. When the sampling rate is increased, such differences are reduced, providing evidence that the benchmark scheme and the proposed scheme display the same dynamics in the limit of infinite sampling rate, and $\forall\ s$.

From this simulation, it is interesting to plot the energy components for the benchmark scheme and for the proposed scheme. This is done in Fig. 5. In accordance to what was noted previously, for $s = 3$ the potential energy is not non-negative, but remains bounded from below and thus stability is guaranteed. When the sampling rate is increased, the minimum of the potential energy tends to zero.

4.3. Cubic Oscillator

Another interesting system is offered by the cubic oscillator, described by an equation of the type

$$\ddot{u} = -\frac{K}{M}u^3, \tag{24}$$

and for which a second-order accurate, unconditionally stable scheme is offered by (see [11])

$$u^{n+1} = \frac{2}{1 + \frac{K}{2M}k^2(u^n)^2}u^n - u^{n-1}. \tag{25}$$

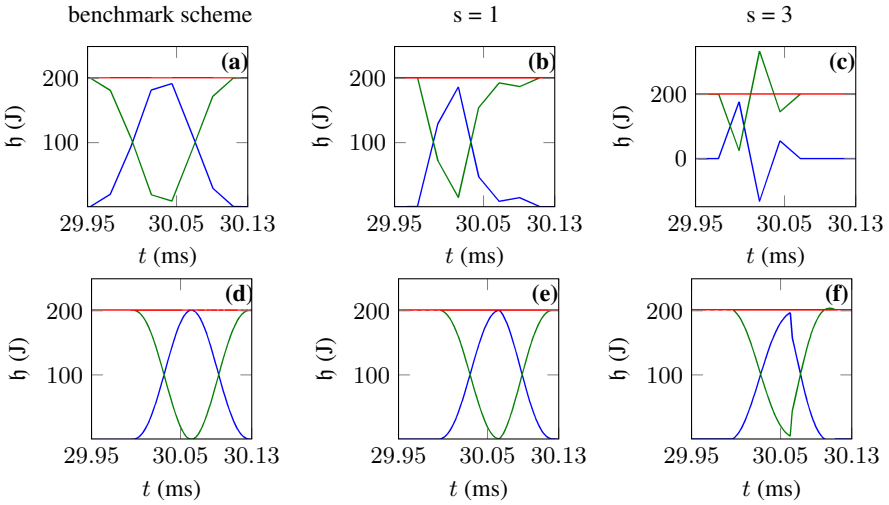

Figure 5: Collision of a fast particle against a stiff barrier, energy components. Comparison of benchmark scheme (23) and proposed scheme, for $s = 1$ and $s = 3$. For all plots, red line is total energy, green is kinetic, and blue is potential. (a)-(c): $f_s = 44100$, (d)-(f): f_s =441000. The energy components are taken from the same simulation as Fig. 4

This benchmark scheme is compared in Fig. 6 to the proposed scheme for various values of s. As in the previous examples, the choice $s = \frac{1}{2}$ gives results that are virtually undistinguishable from the benchmark scheme, with more and more discrepancies as s is increased. As for the case of the simple harmonic oscillator, several spectral peaks appear for $s \neq \frac{1}{2}$ in the higher frequency range, and also the oscillations of the solution in the proposed scheme are a little faster than for the benchmark scheme. With respect to the case of the simple harmonic oscillator, in this case the spectral content of the solution is sensitive to the initial conditions, and in particular the oscillator displays a hardening effect (i.e. shift of the spectrum to higher frequencies for higher initial velocities and displacements). Unlike the case of the simple harmonic oscillator, the spurious spectral peaks appearing in the spectrum for $s \neq \frac{1}{2}$ also display such hardening effect, resulting in some high frequency spectral content which can be quite clearly heard when comparing against the benchmark scheme. Increasing the sampling rate reduces this perceptual effect.

5. CONCLUSIONS

Nonlinear forces, and in particular collisions, are of prime importance for many applications in musical acoustics. In this paper, a novel family of finite difference schemes was presented for collisions in the lumped case, as well as for nonlinear oscillators of any odd power. With respect to previous numerical models, the current scheme requires only the evaluation of a square root at each update, therefore no iterative root finders are needed. The scheme is energy-conserving, and conditions for boundedness of the nonlinear energy can be given in terms a free parameter in the Hamiltonian. The robustness of the algorithm was tested for a large number of cases, showing very good computability properties $\forall \alpha \geq 1$ for a choice of the free parameter $s \geq 1$. The choice of $s = \frac{1}{2}$ gives the most accurate results, however preliminary brute force analysis shows that such case is also the least computable (i.e. the roots of the quadratic are complex in many cases). Although brute force

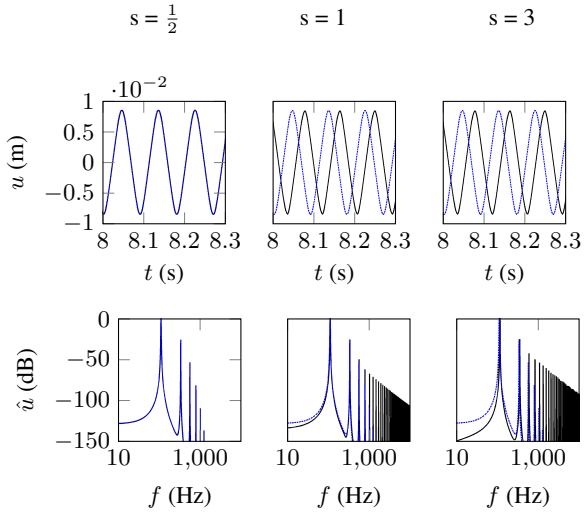

Figure 6: Cubic oscillator. Comparison of current scheme, for potential (3a) with $\alpha = 3$ (solid black line), and benchmark scheme (25) (dashed blue line). Top row: time domain. Bottom row: frequency domain. Free parameter s chosen as indicated on top. Stiffness of the oscillator is $K = 10^{10}$, and mass is $M = 1$ kg. Sampling rate is $f_s = 44100$. Initial conditions: $v_0 = 5$ m/s, $u_0 = 0$ m.

analysis cannot be exhaustive, there is strong evidence that higher values of s do increase the overall robustness of the algorithm, at the expense of accuracy. It is hoped that the current algorithm can be extended to the case of collisions of one lumped and one distributed object (for example, a string and a rattle), for real-time applications.

6. ACKNOWLEDGMENTS

This work was supported by the Royal Society and by the British Academy, through a Newton International Fellowship. Dr Stefan Bilbao is kindly acknowledged for his precious comments on the properties of the scheme.

7. REFERENCES

[1] S. Bilbao, A. Torin, and V. Chatziioannou, "Numerical modeling of collisions in musical instruments," *Acta Acustica united with Acustica*, vol. 101, no. 1, pp. 155–173, 2015.

[2] D. W. Marhefka and D. E. Orin, "A compliant contact model with nonlinear damping for simulation of robotic systems," *IEEE Transactions on Systems, Man, and Cybernetics - Part A: Systems and Humans*, vol. 29, no. 6, pp. 566–572, 1999.

[3] D. Baraff, "Fast contact force computation for nonpenetrating rigid bodies," in *Proceedings of the 21st Annual Conference on Computer Graphics and Interactive Techniques (SIGGRAPH)*, 1994.

[4] P. Wriggers and T. Laursen, *Computational contact mechanics*, Springer-Verlag, Vienna, 2008.

[5] A. Krishnaswamy and J. O. Smith, "Methods for simulating string collisions with rigid spatial obstacles," in *2003 IEEE Workshop on Applications of Signal Processing to Audio and Acoustics*, 2003.

[6] C. P. Vyasarayani, S. Birkett, and J. McPhee, "Modeling the dynamics of a vibrating string with a finite distributed unilateral constraint: Application to the sitar," *The Journal of the Acoustical Society of America*, vol. 125, no. 6, pp. 3673–3682, 2009.

[7] C. Issanchou, J-L. Le Carrou, S. Bilbao, C. Touzé, and O. Doaré, "A modal approach to the numerical simulation of a string vibrating against an obstacle: applications to sound synthesis," in *Proceedings of the 19th Conference on Digital Audio Effects (DAFx-16)*, 2016.

[8] V. Chatziioannou and M. Van Walstijn, "An energy conserving finite difference scheme for simulation of collisions," in *Proceedings of the Stockholm Musical Acoustics Conference (SMAC)*, 2013.

[9] M. van Walstijn, J. Bridges, and S. Mehes, "A real-time synthesis oriented tanpura model," in *Proceedings of the 19th International Conference on Digital Audio Effects (DAFx-16)*, 2016.

[10] S. Bilbao, "Numerical modeling of string barrier collisions.," in *Proceedings of the International Symposium on Musical Acoustics (ISMA)*, 2014.

[11] S. Bilbao, *Numerical Sound Synthesis: Finite Difference Schemes and Simulation in Musical Acoustics*, Wiley, Chichester, UK, 2009.